Dijlah Journal of Medical Sciences (DJMS) Vol. 3, No. 1, January, 2026, pp. 1-13
P-ISSN: 3078-3178, E-ISSN: 3078-8625, paper ID: 01

ORIGINAL ARTICLE

MiR-155 Expression by Real-Time PCR as a New Tool to Diagnose Prostate Cancer as an Alternative to the Traditional ELISA Assay

Hiba Adil Kadhim[1*], Basma Talib Al-Sudani[2], Hadeel Saeed Hadi[3]
[1]Department of Biology, Faculty of Science, Urmia University, Urmia, Iran
[2]College of Pharmacy, Mustansriyah University, Baghdad, Iraq
[3]College of Pharmacy ,University of Kut

Article Info

Article history:

Received August, 22, 2025
Revised September, 17, 2025
Accepted October, 11, 2025

Keywords:

MiR-155,
MRNA PSA,
TPS,
CEA

ABSTRACT

Prostate cancer is a common malignancy in men, and early detection is essential for effective treatment. While PSA is the most used biomarker, its limitations call for better diagnostic tools. This study aimed to evaluate the diagnostic potential of miR-155 expression using real-time PCR as an alternative to traditional ELISA-based markers such as PSA, TPS, and CEA. Blood samples were collected from 80 prostate cancer patients and 80 healthy controls at Al-Andalus Specialist Hospital. Serum miR-155 and blood PSA mRNA levels were measured using real-time PCR. Additionally, ELISA assays were used to assess PSA, TPS, and CEA levels. The expression of miR-155 and PSA mRNA was significantly higher in patients than in controls (3.8-fold and 1.7-fold, respectively; $p < 0.0001$). MiR-155 showed an AUC of 97% for sensitivity and specificity, outperforming PSA mRNA (AUC 89%). ELISA results also indicated elevated levels of PSA, TPS, and CEA in patients, but miR-155 was the most reliable biomarker. MiR-155 demonstrated superior diagnostic performance compared to traditional markers due to its high sensitivity, specificity, and cost-effectiveness, suggesting its potential as a powerful and practical tool for prostate cancer detection.

Corresponding Author:

* Hiba Adil Kadhim
Department of Biology, Faculty of Science, Urmia University, Urmia, Iran
Email: hibaadil235@gmail.com

1- INTRODUCTION

Prostate cancer or carcinoma of the prostate is the development of cancer in the prostate a gland in the male reproductive system [1]. Early detection of prostate cancer is crucial for effective treatment, and diagnosis often involves a combination of clinical examinations, imaging, and biomarker testing. Biomarkers can be used to diagnose, in the assessment of disease severity, stratify risk, predict and guide clinical decisions, and guide treatments and responses to them. MicroRNAs are natural small RNAs that control gene expression. There is overwhelming evidence that the expression of miRNAs is altered in human cancer by multiple mechanisms: miRNA gene amplifications or deletions, abnormal control of the transcriptional machinery, dysregulated epigenetic changes, and malfunction of the machinery involved in the biogenesis of miRNAs. MiRNAs are either considered to be oncomiRNAs or to have tumor-suppressing properties in specific situations. These miRNAs that are deregulated have been observed to affect prominent pathways in cancer that involve maintaining proliferation, avoiding growth suppression, resisting death, and causing invasion and metastasis. Increasing research demonstrated that miRNAs are likely to be used as biomarkers for the diagnosis, prognosis, and treatment of human cancers that are still in the early stages of development [2]. Bioinformatics tools offer a new approach to finding miRNAs that are significant in the development of PCa, but large scale studies that seek to choose a miRNA profile are time-consuming and expensive. As a new approach to describing new biomarkers

for PCa, the majority of research to date has been conducted in serum or plasma to assess the practicality of miRNAs in terms of clinical diagnosis. Determining the value of miRNAs in the treatment of PCa will necessitate additional efforts. miR-155 is a powerful tumor-suppressing miRNA and has a significant impact on miRNAs. It's created during the process of B-cell cluster's processing, has been observed to be over expressed in multiple cancer types, and is associated with the onset of leukemia, breast cancer, and lung cancer [3, 4]. However, it is still unclear how miR-155 functions biologically and how exactly it treats prostate cancer. miR-155 was demonstrably elevated in four different prostate cancer cell lines (DU145, LNCaP, 22RV1, and PC-3) [5]. Additionally, the inhibitor of miR-155, when transfected into human prostate cancer cells, decreased their proliferation rate, this suggests that miR-155 promotes the growth of these cells in vitro. Additionally, the effect of miR-155 on the distribution of the cell cycle and the degree of cell death in cancer cells of the prostate was studied. The procedure of scheduled cell death called apoptosis is crucial to the cellular growth and conservation.. Cell cycle checkpoints ensure the fidelity of cell division by precisely regulating the activities of the cell cycle. However, the percentage of cells in the G1 phase that are arrested is higher after transfection than it is for the S phase, and the decrease in the latter is greater. This is initiated by multiple causes that cause cell death and apoptosis [6, 7]. It was shown that decreased expression of miR-155 caused cell cycle arrest. These results suggested that miR-155 could be a molecular target for prostate cancer early diagnostic and prognosis indicators. According to that, this study aims to investigate the ability of miR-155 levels to diagnose prostate cancer and compare the results obtained from the miR-155 assay with the conventional detection assays for blood PSA mRNA and serum PSA, TPS, CEA. To conclude, miR-155 performed exceptionally well when compared to many other diagnostic biomarkers for prostate cancer due to their high sensitivity and specificity. miR-155 test provides significant advantages over traditional PSA by RT-PCR and ELISA as well as TPS and CEA by ELISA through ease of use and wide application for other biomarkers. So, it can be considered that MiR-155 is the most useful biomarker for prostate cancer diagnosis.

2- MATERIALS AND METHODS

2.1 Materials

TRIZOL and Qiagen's miRNeasy Serum/Plasma Kit were purchased from Qiagen, USA. QuantiFluor® RNA system was purchased from Promega, Germany. PSA, TPS, and CEA enzyme-linked immunosorbent assay (ELISA) kits were purchased from Elabsciences, USA. A reverse transcription kit was purchased from Bioneer, Korea. The microplate reader was purchased from BioTek, USA. RT-PCR was purchased from Bioneer, Korea. Primer's sequence was provided by Bioneer, Korea. Other common reagents were purchased from Thermo Scientific, USA.

2.2 Primers sequence

Table (1): Primer sequences used to amplify different genes by polymerase chain reaction (PCR)

Genes	Forward Primers (5'-3')	Reverse primers (5'-3')	Supplier
PSA	CATGGTATGATGGACC	TTCGAAGTCGCACAGCAGCT	BioNeer- Korea
miR-155	CGATGGTATATGGACC	TTCGAGCCGATACAGCAGCT	BioNeer- Korea
GAPDH	ACCAGGTATCTGCTGGTT	TAACCATGATGTCAGGTGGTT	BioNeer- Korea

2.3 Sample collection

Pre-operative blood was obtained from 80 men with prostate cancer who had been verified histologically for this study between April 2022 and July 2023 at the Al-Andalus Specialist Hospital in Baghdad, Iraq. Retrospective data collection included gathering patient information such as age = 54±3 (median ±SD). Patients with serious infections, ongoing clinical illnesses, or a background of any other cancer were not allowed to participate. Docetaxel was used as the adjuvant chemotherapy (Taxotere). Radiologists evaluated these patients' therapeutic responses under World Organization (WHO) standards. In addition, serum from a group of 80 healthy outpatients at a private lab was taken. The participants were all Iraqi descent. No healthy controls have previously been diagnosed with any cancers. The average age of these healthy individuals is 53.2±2. There is no significant difference in the age of the prostate cancer patients and the controls (p=0.7899, Mann-Whitney U test). 10 ml blood sample (3 ml whole blood for the mRNA PSA and 7 ml for the serum) will be collected in a container with polymer gel and a clot activator. The serum's content, after coagulating at a temperature of 30 degrees Celsius for 60 minutes, was then centrifuged at a speed of 1300 g for 15 minutes. The supernatant was then re-centrifled at 10,000 g for 10 min at 4C°, this time; all of the cellular debris was removed. The serum was divided into small tubes that were microcentrifuge, and these were stored at - 20 degrees Celsius until they are used.

2.4 Methods

Firstly, high-quality RNA was isolated from blood and sera using the protocol that combines both TRIZOL reagent and QIAamp RNA Blood Mini Kit for mRNA PSA and miRNeasy Serum/Plasma Kit for miR-155 from Qiagen [10]. According to the RNA from blood, the QIAamp RNA simplifies the isolation of RNA from blood with a fast spin-column procedure. Red blood cells are selectively lysed and white cells are collected by centrifugation. White cells are then lysed using highly denaturing conditions which immediately inactivate RNases. After the sample washomogenized using the QIA shredder's spin column, it was transferred to the QIAamp column. Total RNA is associated with the QIAamp membrane, and contaminants are removed, leaving only pure RNA to be eluted in 30-100 µl of RNase-free water. About the miRNA in the serum, the prepared serum is derived from the freezed samples.. Then, added 5 volumes QIAzol Lysis Reagent to the sample (200 µl sample + 1 ml QIAzol Lysis Reagent). Vortexed and incubated the mixture at a temperature of 25°C for 5 minutes. 200 ml of chloroform were added to the starting sample (200 ml) and the cap was securely attached. Shacked for 15 seconds and then incubated at room temperature for 2-3 minutes. RNA remained confined to the aqueous phase. After that, the supernatant was decanted for 15 minutes at 12,000 x g at 4°C. Moved the top aqueous layer to a new container. Avoid any form of transfer. Increased the volume of the first 1.5 parts by 100% (600 µl of the aqueous phase plus 900 µl of the ethanol). Pipet everything together. Transfer up to 700 µl of the sample, including any crystals, to the RNeasy MinElute spin column that is placed in a 2 ml collection tube. Close the lid and rotate the centrifuge at a speed of ≥8000 x g for 15 seconds at a temperature of room. Forgo the flow-through, repeat the procedure with the remaining portion of the sample. Add 700 ml of the RNeasy MinElute spin column to the 700 µl Buffer RWT. Close the lid, and centrifuge for 15 seconds at a minimum of 8000 x g. Discard the flow-through. Pipet 500 µl of Buffer RPE into the RNeasy MinElute spin column. Close the lid, and centrifuge for 15 seconds at a minimum of 8000 x g. Then, discard the flow-through. Add 500 ml of 80% ethanol to the RNeasy MinElute spin column. Close the lid, centrifuge for 2 minutes at a minimum of 8000 x g, discard the flow-through and the collection tube. Place the RNeasy MinElute spin column in a new 2 ml collection tube. Top speed for 5 minutes, then decrease the speed to a low setting, this will allow the membrane to dry. Additionally, the collection tube should be discarded and the RNeasy MinElute column placed into a new 1.5 ml collection tube. Directly added 14 µl of RNase-free water to the center of the spin column's membrane and then centrifuged for a total of 1 min at full speed to release the RNA. Ultimately, the volume and quality of isolated RNA was assessed with the Quantus Fluorometer's Nanodrop. [8]. Next, reverse transcription was used to convert the miRNA's RNA to DNA. 500ng of miRNA, 1ml of dNTPs (10mM each dNTP), 250ng of random primers (0.5ug of random primers per µg of miRNA), and 14ml of free water were added to a reaction vessel. This mixture was incubated at 70 degrees Celsius for five minutes, then immediately placed on ice for the annealing of random nucleotides. Next, 4µl of the reverse transcription buffer (5 x), 1µl of the M-MLV reverse transcriptase, and 1µl of the RNAse inhibitor (RNAse out) were incorporated into the mixture. Afterward, the reaction was incubated at 16°C for 30 hours for the first round of transcription, followed by 30 minutes at 42°C and a final heat inactivation of the enzyme for 5 minutes at 85°C. Then, the reaction was maintained at 4C° [9]. Third, quantitative real-time PCR (qPCR) was conducted on the MiniOpticon Thermoycler. For the detection of amplified DNA in real time, the Taqman method with hydrolysation probes was employed. As a result, a DNA molecule with a fluorescent tag at the 5’ end and a TAMRA tag at the 3’ end was used. Both dyes have a propensity to consume each other when located near each other. The order of this investigation's sequence was intended to allow it to attach to the DNA substrate between forward and reverse primers. Now, during the process of DNA's amplifiability, the 5' exonuclease activity of the polymerase enzyme causes the degradation of an annealed probe, this results in the release of both fluorescent dyes, thereby quenching is no longer present. Fluorescence is considered a signal of increase [10]. The outcomes of the qPCR are fluorescence graphs of the various genes, which are dependent on the number of genes or transcripts present.

The expression of miRNAs was compared to the level of Cel-Mir-39. The copy number of genes or their transcripts was compared to a reference gene using the 2-ΔΔCq method. As a result, the –ΔCp value was determined as in Equation 1. Next, the 2-ΔCp value was determined as in Equation 2. This indicates the number of relative genes and their transcript levels in comparison to the reference gene at a presumed efficiency of 100% during PCR. The 2-ΔΔCp value, according to Equation 3, is employed to contrast two genes from the same sample. Equation 1: Compute the difference inCp values between the reference gene and the miRNA's target gene for the 145th and the GAPDH gene for the mRNA PSA.

$-Cq = Cq_{cel-mir-39} - Cq_{gene}$	(1)
for miR-155	
$-Cq = CqGAPDH - Cq_{gene}$	(1)
for PSA	

Equation 2: The ratio of the gene's copy number to its transcript in relation to Cel-mir-39.

$\frac{gene}{cel-mir-39} = 2^{-Cp}$	(2)
for miR-155	
$\frac{gene}{GAPDH} = 2^{-Cp}$	(2)
for PSA	

Equation 3: The ratio of the gene's copy number to its transcript in one sample relative to the same gene in another sample.

$\frac{G_{sample1}}{G_{sample2}} = \frac{2^{-Cp_{G1}}}{2^{-Cp_{G2}}}$	(3)

4.5 Serum TPS, CEA, and PSA Assays using Enzyme-Linked Immunosorbent Assay

To assess the degree to which human serum contains tissue polypeptides that are specific to humans, CEA, and PSA, the authors utilized three different methods. The concentrations of TPS, CEA, and PSA were determined using the ELISA method according to the instructions of the manufacturer, USA.

The GraphPad Prism 8.0, which is used to conduct all statistical evaluations, was employed to do this. The levels of serum miRNAs were compared by t tests. To assess the accuracy of the diagnosis, we conducted a receiver operating characteristic (ROC) analysis of the data. The total area under the ROC (AUC) was then calculated. Any P value that resulted in a value less than 0.05 was considered significant.

3- RESULTS

The resulting curves of gene expression level of miR-155 are shown in Fig. 1.
The fold change was calculated using the Livak method [8]. Table 1 showed the effect of miR-155 on cancer patients in terms of the relative amount of miR-155 based on the spiked-in cel-mir-39 as a comparison. The results demonstrated that the percentage of cells expressing miR-155 was significantly higher in patients with prostate cancer than in controls (3.8 $p<0.0001$; Fig.2).

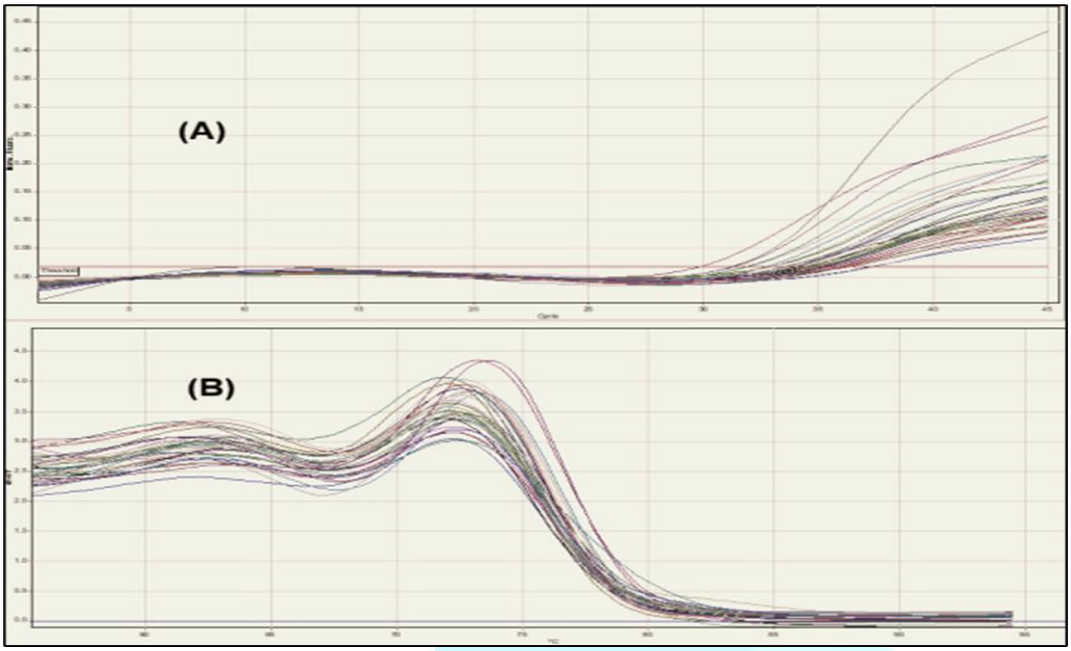

Figure (1): Rt-PCR results of related MicroRNA expression tested by threshold cycle (Ct). (A) Gene amplification. (B) Gene dissociation curves

Table (2): The expression of the miR-155 gene in patients with PC and controls

miRNA	mean ΔCt ±SE (Controls)	mean ΔCt ±SE (PC patients)	p-value	ΔΔCt	Fold expression
miRNA-155	27.57± 1.32	25.6± 1.42	p<0.0001	-1.97	3.8

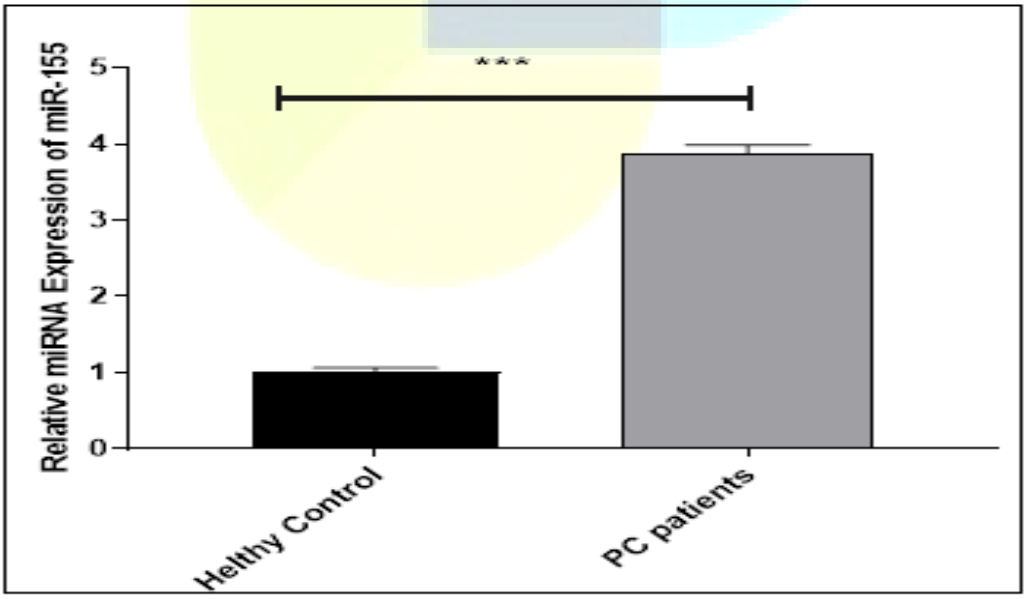

Figure (2): The levels of serum miR-155 in controls with normal functioning (n = 80) and patients with prostate cancer (n = 80). are compared

The percentage of expressed miR-155 was adjusted to match the amount of spiked-in cel-mir-39. The line is the average±standard deviation. The difference that was significant was determined using t-tests. The outcome demonstrated a higher percentage of miR-155 in prostate cancer patients than in controls ($p<0.0001$).

Fiigure 3 demonstrates the investigation of the diagnostic value of miR-155 utilizing the receiver operating characteristic (ROC) curve, the areas under the ROC curve were 0.9458 (95% CI: 0.909 to 0.9823). The results of AUC (the area under the ROC curve) indicated that the study had a useful marker that could be used to differentiate cases from controls, the optimal sensitivity and specificity were both 97%.

mRNA PSA was evaluated. As shown in Table 3 and Figure 3, blood mRNA PSA levels were significantly increased by 1.7 in prostate cancer as compared with normal controls ($p<0.001$). The relative expression level of mRNA PSA was normalized to GAPDH. Sensitivity and specificity were both 97%.

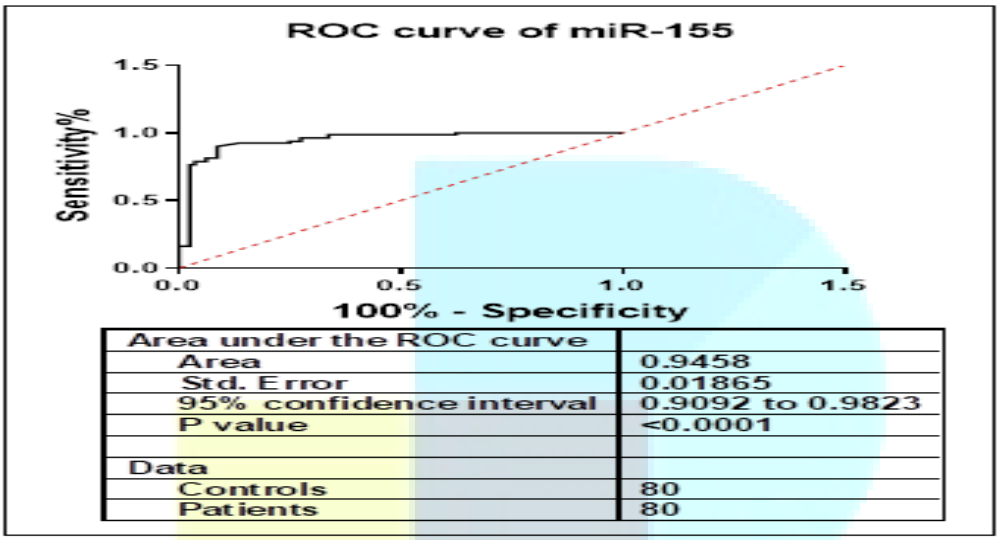

Figure(3): The receiver operating characteristic (ROC) analysis for the diagnostic value of miR-155 is described The AUC (the total area under the ROC) was 0.9458 (95% CI: 0.909 to 0.9823)

To compare the results of miRNA-155 as a diagnosis of prostate cancer, the expression of

Table (3): mRNA PSA gene expression in PC patients and control

miRNA	mean ΔCt ±SE (Controls)	mean ΔCt ±SE (PC patients)	p-value	ΔΔCt	Fold expression
mRNA PSA	45.3± 1.5	44.5± 1.87	p<0.001	-0.8	1.74

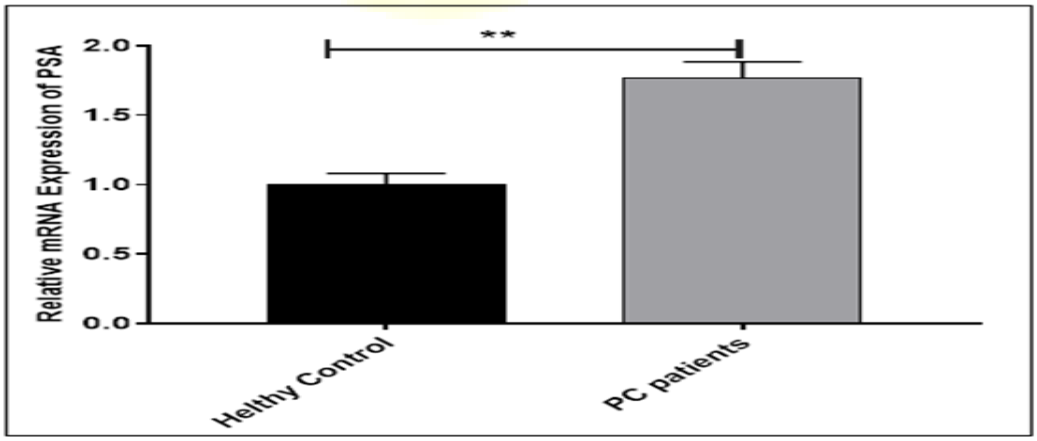

Figure (4): Blood's mRNA for PSA was measured in normal controls (n = 80) and prostate cancer patients (n = 80)

The relative amount of mRNA PSA was compared to the level of GAPDH. The line is the average±standard deviation. A significant difference was determined using t-tests. The results showed that patients with prostate cancer have higher levels of mRNA PSA.

Using the receiver operating characteristic (ROC) curve, assess the value of the PSA in diagnosing disease. According to the figure, the AUC (the total area under the ROC) was 0.8457 (95% CI: 0.7711 to 0.9203). The study of AUC demonstrated that PSA was a significant marker for differentiating cases from controls, the value of this marker was 0.8457 (95% CI: 0.7711 to 0.9203) p >0.0001). The optimal degree of sensitivity and specificity was 89%.

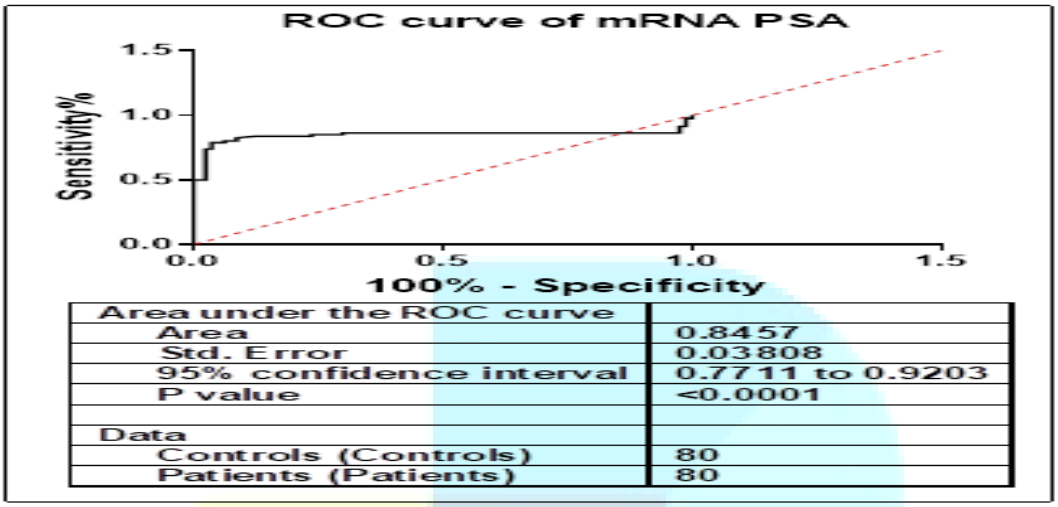

Figure (5): The ROC (Receiver operating characteristics) analysis of the diagnostic value of mRNA PSA gave an AUC (the area under the ROC curve) of 0.8457, with a 95% CI that spanned from 0.7711 to 0.9203

The serum levels of Tissue Polypeptide Specific Antigen TPS in prostate cancer patients compared to healthy participants ($p<0.0001$, t-test), Table 3, and Figure 6.

Table(4): Serum Concentrations of TPS in patients with prostate cancer and healthy control

Diagnosis	No. of patients	TPS (U/liter)		
		Median	Range	No. > 100 U/liter (%)
Healthy Control	80	96	89–101	3(3.75)
Prostate Cancer Patients	80	438.7	119–605	80(100)

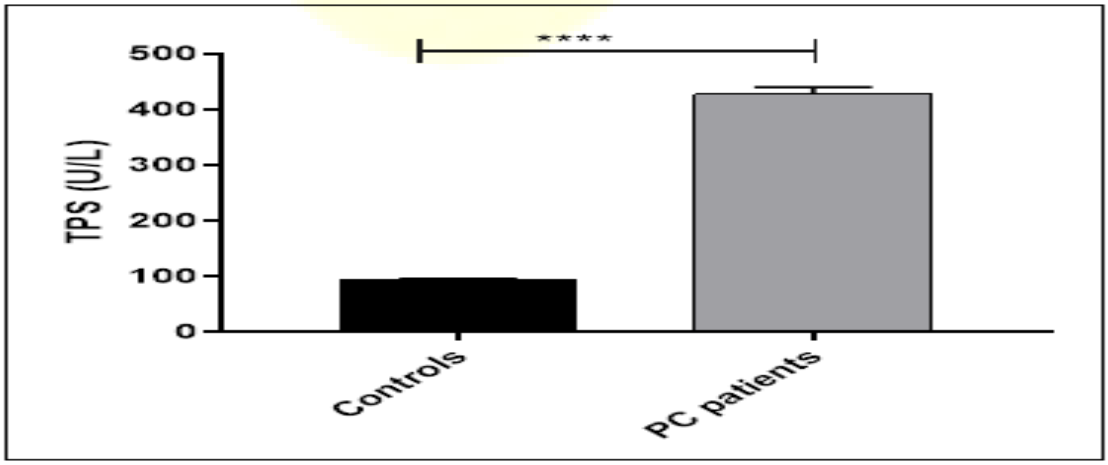

Figure (6): Changes in serum TPS levels for prostate cancer patients as against control has been represented by the Median±SE value. Statistically significant differences have been worked out using unpaired t-tests (two-tailed). The result revealed a higher level of TPS in prostate cancer patients (p<0.0001)

Fig. 7 shows the ROC (receiver operating characteristics) analysis for diagnosis using TPS. AUC (the area under the ROC curve) came to 0.8625, within a 95% confidence interval from 0.787 to 0.938.

The quantity of Carcinoembryonic Antigen CEA in the patients with prostate cancer and controls was also assessed. The serum concentrations of CEA were significantly higher than the healthy controls as demonstrated in the Table 4, Figure 8.

Figure 9 shows the receiver operating characteristics (ROC) curve analysis for the diagnostic value of CEA. The AUC (the area under the ROC curve) was 0.8995 (95% CI: 0.8452 to 0.9537).

Table (5): Serum levels of CEA in patients with prostate cancer and healthy control

Diagnosis	No. of patients	CEA (ng/ml)		
		Median	Range	No. > 3.5 ng/ml (%)
Healthy Control	80	2.3	1-3.5	0(0)
Prostate Cancer Patients	80	24.9	12-30	80(100)

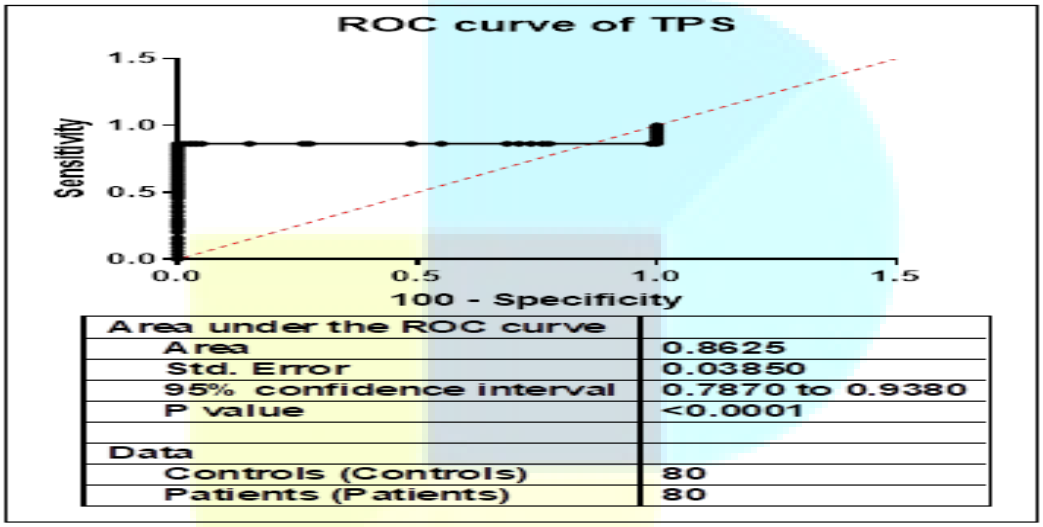

Figure (7): The method of operating characteristic (MO) analysis for the diagnostic value of TPS is explained. The total area under the ROC was 0.8625 (95% CI: 0.787 to 0.938)

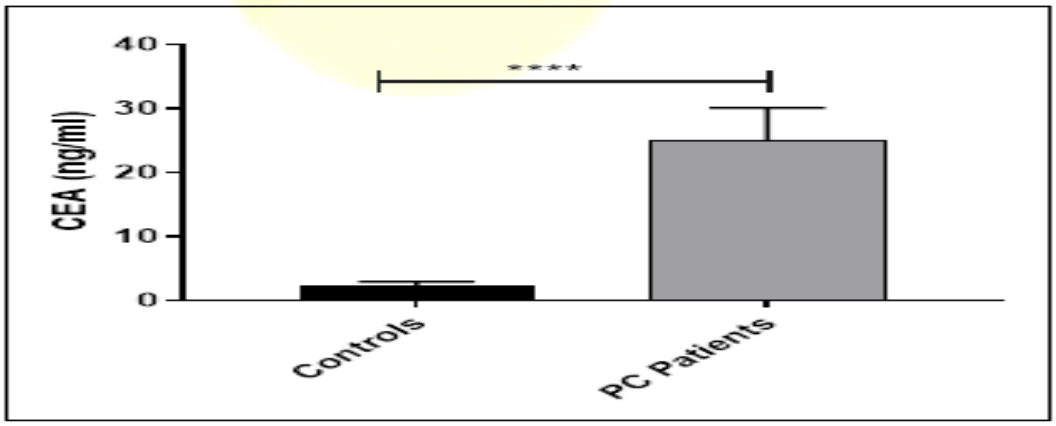

Figure (8): Variations in CEA values for prostate conditions against control. The line stands for Median±SE value. A statistical test used to find the significant difference was an unpaired t-test (two-tailed). This brought out that raised levels of CEA were found in patients with prostate cancer, p<0.0001

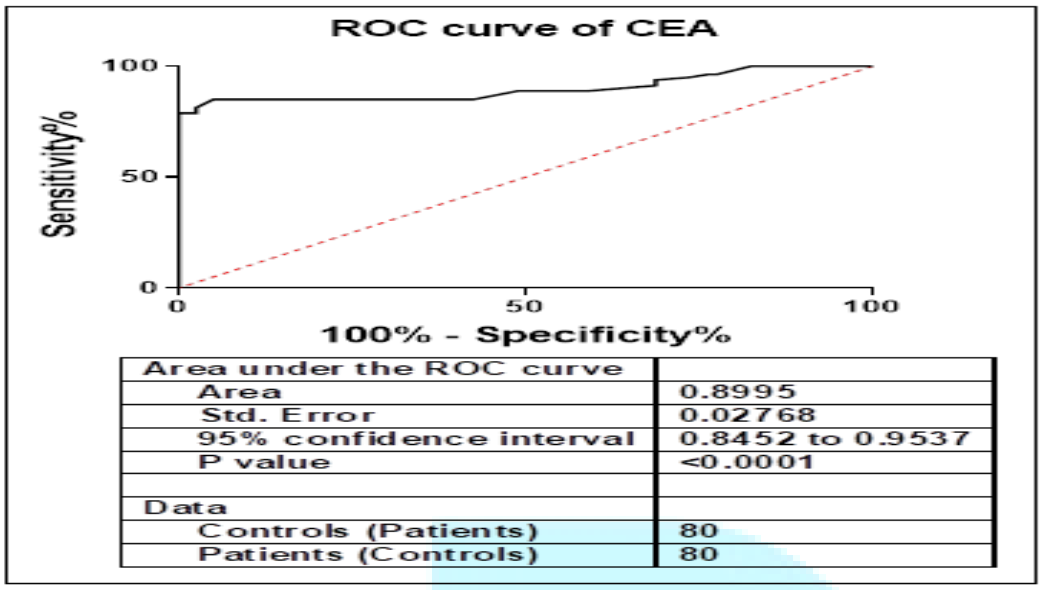

Area under the ROC curve	
Area	0.8995
Std. Error	0.02768
95% confidence interval	0.8452 to 0.9537
P value	<0.0001
Data	
Controls (Patients)	80
Patients (Controls)	80

Figure (9): Receiver operating characteristic (ROC) analysis of the diagnostic value of CEA: AUC (total area under ROC) was 0.8995 (95% CI: 0.8452-0.9537)

PSA are frequently used assays for monitoring diseases of prostate cancer. Table 5 and Fig. 10 illustrate the increased level of serum PSA prostate cancer by 13.2 ng/ml as compared with 2.7 ng/ml in healthy control.

Table (6): Serum levels of PSA in patients with prostate cancer and healthy control

Diagnosis	No. of patients	PSA (ng/ml)		
		Median	Range	No. > 4 ng/ml (%)
Healthy Control	80	2.7	1.5-4	0(0)
Prostate Cancer Patients	80	13.2	4.5-19	80(100)

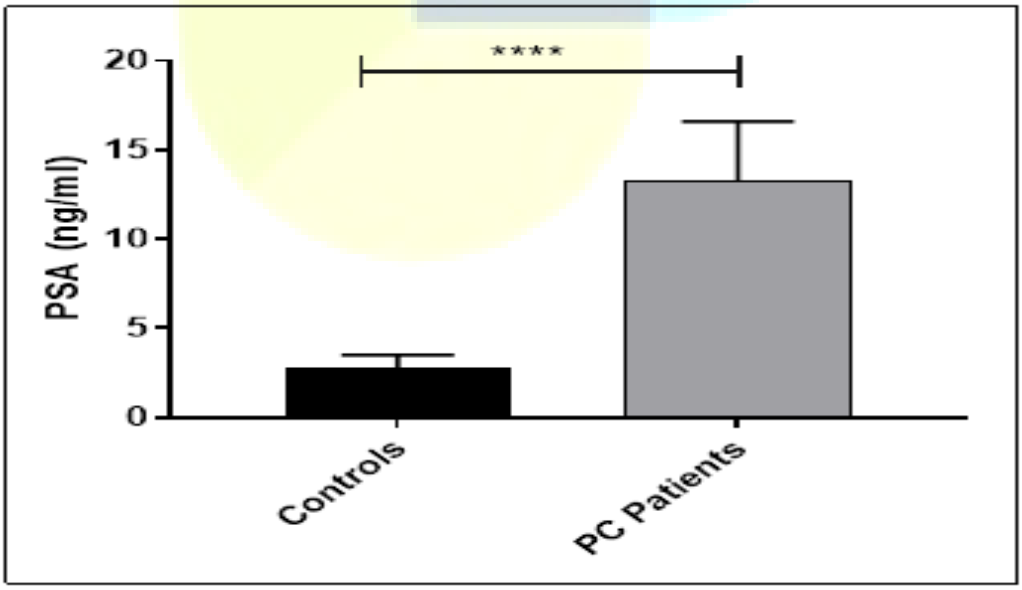

Figure (10): Changes in serum PSA levels for prostate cancer patients compared to control. The line represents the Median±SE value. The statistically significant difference was determined using unpaired t-tests (two-tailed). The result revealed a higher level of PSA in prostate cancer patients (p<0.0001)

As a diagnosis, the results of receiver operating characteristics (ROC) curve analysis for PSA demonstrated that the area under the ROC curve was 0.8705 (95% CI: 0.8072 to 0.9339) as shown in Fig. 11.

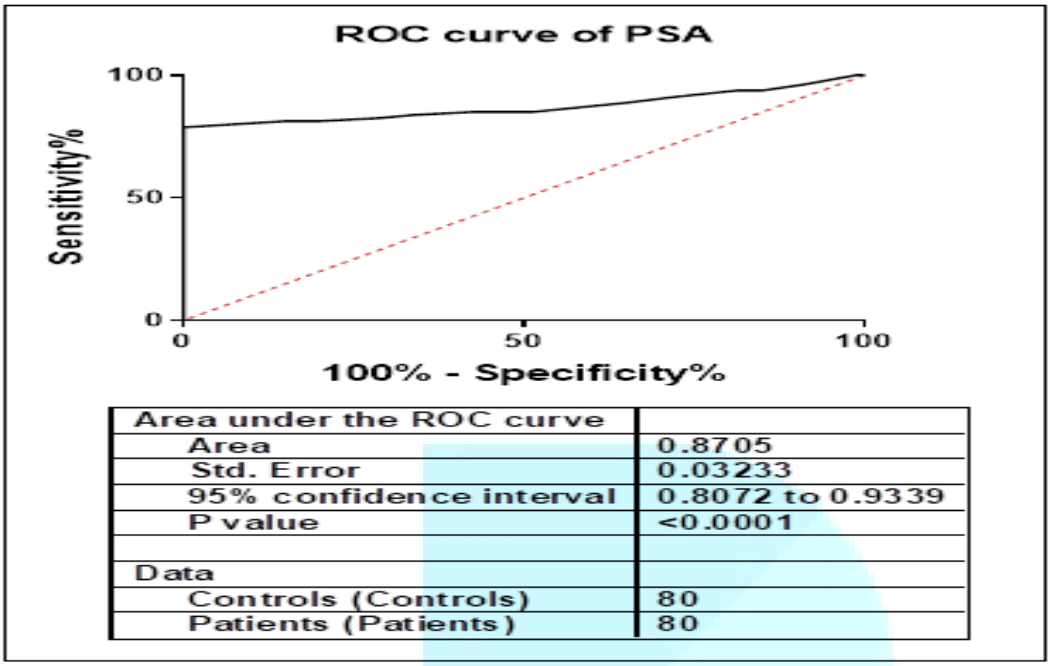

Area under the ROC curve	
Area	0.8705
Std. Error	0.03233
95% confidence interval	0.8072 to 0.9339
P value	<0.0001
Data	
Controls (Controls)	80
Patients (Patients)	80

Figure (11): The receiver operating characteristic (ROC) analysis for the diagnostic value of PSA is described as follows. The AUC (the total area under the ROC) was 0.8705 (95% CI: 0.8072 to 0.9339)

4- DISCUSSION

Diagnosis of PCa and proper staging have a crucial value in clinical management and patient care. Despite great advances in biology and imaging, the major pillars still remain the basics as we depend on a rec- tale examination and blood test for prostate-specific antigen (PSA) multiparametric magnetic resonance imaging (mpMRI) for local staging. However, the general nature of the PSA's recommendations for PCa, the creation of screening programs, and the fact that over 60% of PCas are diagnosed in patients that are symptomatic, with no abnormal DRE and a high PSA. Total PSA (tPSA) continues to be the primary platform for biological experiments in this evolving landscape of tumor markers, as documented in a recent comprehensive review [12]. High PSA levels are associated with a higher risk of prostate cancer. Unfortunately, PSA levels are organ-specific, not prostate cancer-specific. This leads to a correlation between the prevalence of benign prostatic hyperplasia (BPH) and prostate cancer. A high PSA value is associated with a higher probability of PCa. Sadly, to state, PSA is specific to the organ, and not specific to prostate cancer. This causes a correlation between BPH and PCa in their prevalence. At the same time, the PCa prevention trial (PCPT) study demonstrated that PCa can be detected even if PSA is below 4 ng/mL, pointing out the fact that there is no PSA cut-off threshold below which the risk of detecting a PCa on biopsy is zero. The choice of a PSA threshold at which a clinician might recommend a biopsy remains controversial. This requires the urologist a thorough explanation regarding the respective risks and benefits of the procedures and the possible utilization of other biological markers. The potential benefit of the PSA test for the detection of prostate cancer is that it can diagnose the disease early on, before it has spread, this would allow for a more lenient treatment approach that would still allow for a controlled death rate due to the disease. Systematic reviews and meta-analyses of all of the randomized controlled trials that compared PSA detection with standard care in men without a diagnosis of prostate cancer were conducted. The results showed that over the course of a decade, the screening of PSAs for prostate cancer does lead to a small decrease in the mortality associated with the disease [13]. The harm that accrues from its potential benefit is significant. The cancers that it helps detect grow at a snail's pace such that they would never manifest symptoms or become life-threatening- treatment can harm. This is referred to as overdiagnosis- overtreatment, and the tumors did not pose any threats within one's lifespan. Early detection of prostate cancer does not always equate to being saved. Though the PSA test may be able to pick on smaller tumors within the prostates, some of these small tumors have most probably already spread outside the prostate by the time it is detected and may prove uncurable. The PSA test gives negative-positive results. A positive result for a test in which no cancer exists but the PSA level is high constitutes a false positive. A false positive will create anxiety

and probably lead to more medically harmful procedures, for example, biopsy in search of cancer, among others. Biopsy may result in a dangerous infection, or pain, or bleeding. False-positive test results are common with PSA screening, about 6%-7% of men on any given round of screening have a false-positive PSA test, and since only about 25% of men who have biopsies due to an elevated PSA level are found to have prostate cancer [14]. However, the decreased or suppressed production of the antigen in about 10-15% of patients with prostate cancer is detrimental to the diagnostic accuracy of serum PSA [15]. Also, the exact percentage of PSA in the clinical staging is not known because the majority of the prostate cancer cases are composed of high levels of PSA production [16]. Tissue polypeptide-specific antigen (TPS) is a chemical indicator obtained by immunological mapping of TPA and selecting monoclonal antibodies that recognize specific epitopes of the M3 molecule [17]. Data suggest its clinical usefulness in diagnosis and prognostic assessment of prostate cancer [18]. So, the researcher found that the Tissue Polypeptide-Specific Antigen (TPS) test is associated with the PSA test, and these two tests are useful at the time of diagnosis of prostate cancer [19] as well as the CEA, a protein normally produced during fetal development but often reactivated in certain cancers, is an indicator of whether cancer is growing and spreading or diminishing with treatment. Both CEA and TPS methods provide clinicians with valuable insights into cancer progression, response to therapy, and overall patient management, contributing to more informed medical decisions and improved patient care. Therefore, a development diagnostic method must be found that mimics genetic evolution to diagnose prostate cancer and is more sensitive and accurate in the results. Bioinformatics tools provide a new method to choose miRNAs that are important in the development of PCa, but large-scale studies that screen for miRNAs in bulk are slow and expensive. As a new approach to describing new biomarkers for PCa, the majority of research to date has been conducted in serum or plasma to assess the practicality of miRNAs in terms of clinical diagnosis. Determining the value of miRNAs in the treatment of PCa will necessitate additional efforts. MicroRNAs are a subculture of small nucleic acids that are classified as miRNAs (21–25 nt), non-coding RNAs, which control their target gene expression at the post-transcriptional level [20, 21]. MiRNAs act on gene expression by binding to the 3'-untranslated region (3'UTR) of the target mRNAs, resulting in mRNA cleavage and translational inhibition, thereby down-regulating target protein expression [22]. miRNA dysfunction may contribute to a variety of human diseases, including cancer [46] their role as a cancerous gene or gene that combats cancer, respectively, based on their intended goals. The miR-155 gene is located on chromosome 21q21 and is surrounded by a region called the B cell integration cluster (BIC), which is composed of three different exons and encompasses a distance of 13 kb [23]. The human BIC gene is activated by promoters that are inserted into it, and it has a limited open reading frame. [23]. miR-155 is a common miRNA that possesses multiple functions, it is overexpressed in the majority of human solid tumors of the breast [24], lung cancer [25], thyroid tumor [26], and pancreatic cancer [27]. Recent clinical pathological data indicate that miR-155 is involved in the development of tumors and the diagnosis or prognosis of the disease. The experimental evidence available demonstrates that miR-155 promotes the growth of some tumors, invasion, and metastasis through downstream targets like SHIP1 INPP5, which is deduced by the level of expression in normal versus cancerous tissues. C/EBPbeta , and SOCS1 . All of these lines of evidence indicate that miR-155 is an oncomiR in human cancer. The mechanisms of miR-155 functions as an oncomiR are largely unknown and still unclear how miR-155 functions biologically and how exactly it treats prostate cancer. This study investigated the ability of miR-155 levels to diagnose prostate cancer and tried to compare it with many other diagnostic biomarkers for prostate cancer. miR-155 was demonstrably elevated in four different prostate cancer cell lines (DU145, LNCaP, 22RV1, and PC-3) and prostate cancer tissues [6]. Additionally, the inhibitor of miR-155, when transfected into human prostate cancer cells, decreased their proliferation rate, this suggests that miR-155 promotes the growth of these cells in vitro. On the other hand, several stimuli that cause cell death and apoptosis also prevent the cell from continuing to cycle. . Another investigation demonstrated that downregulation of miR-155 led to cell cycle arrest by targeting multiple anti-apoptotic factors, this caused cell death [6, 7].

5- CONCLUSION

Among the array of biomarkers scrutinized, miR-155 surfaced as the most potent diagnostic tool for prostate cancer. This discovery not only underscores the potential clinical relevance of miR-155 as a distinguishing biomolecular feature but also highlights the significance of exploring miRNA-based mechanisms in the domain of cancer diagnostics and therapeutic interventions. These findings collectively reinforce the imperative for continued exploration of miRNA and related biomolecules to enhance our understanding of prostate cancer pathogenesis and refine diagnostic and prognostic methodologies.

REFERENCES

[1] Rocha, J. M., & Pereira, B. A. G. J. (2019). Biological principles and clinical application of positron emission tomography-tracers in prostate cancer: A review. Prostate International, 7(2), 41–46. https://doi.org/10.1016/j.prnil.2018.12.001

[2] Lameka, K., Farwell, M. D., & Ichise, M. (2016). Positron emission tomography. In Handbook of Clinical Neurology (Vol. 135, pp. 209–227). Elsevier.

[3] Jung, J. H., & Ahn, B. C. (2018). Current radiopharmaceuticals for positron emission tomography of brain tumors. Brain Tumor Research and Treatment, 6(2), 47–53. https://doi.org/10.14791/btrt.2018.6.e7

[4] Wu, Z., Wang, L., Li, Y., Dai, S., & Zhang, D. (2022). Head CT image segmentation and three-dimensional reconstruction technology based on human anatomy. Computational Intelligence and Neuroscience, 2022(1), 7091476. https://doi.org/10.1155/2022/7091476

[5] Tsuyoshi, H., & Yoshida, Y. (2017). Diagnostic imaging using positron emission tomography for gynecological malignancy. Journal of Obstetrics and Gynaecology Research, 43(11), 1687–1699. https://doi.org/10.1111/jog.13436

[6] Rong, J., Haider, A., Jeppesen, T. E., Josephson, L., & Liang, S. H. (2023). Radiochemistry for positron emission tomography. Nature Communications, 14(1), 3257. https://doi.org/10.1038/s41467-023-36377-4

[7] Zhang, J., Traylor, K. S., & Mountz, J. M. (2020). PET and SPECT imaging of brain tumors. Seminars in Ultrasound, CT and MRI, 41(6), 530–540. https://doi.org/10.1053/j.sult.2020.08.007

[8] Hindson, B. J., Ness, K. D., Masquelier, D. A., Belgrader, P., Heredia, N. J., Makarewicz, A. J., et al. (2011). High-throughput droplet digital PCR system for absolute quantitation of DNA copy number. Analytical Chemistry, 83(22), 8604–8610. https://doi.org/10.1021/ac202028g

[9] Balzano, F., Deiana, M., Dei Giudici, S., Oggiano, A., Baralla, A., Pasella, S., et al. (2018). miRNA stability in stored serum samples: A first step toward miRNA-based diagnostic tests for cancer. International Journal of Molecular Sciences, 19(6), 1706. https://doi.org/10.3390/ijms19061706

[10] Brown, A. J., Zhang, Y., Angel, T. E., Watson, M. A., Hummon, A. B., & Caprioli, R. M. (2020). Advances in mass spectrometry-based spatial proteomics: Software and workflows. Journal of Proteome Research, 19(11), 4407–4415. https://doi.org/10.1021/acs.jproteome.0c00539

[11] Fendler, A., Stephan, C., Yousef, G. M., Kristiansen, G., & Jung, K. (2016). The translational potential of microRNAs as biofluid markers of urological tumours. Nature Reviews Urology, 13(12), 734–752. https://doi.org/10.1038/nrurol.2016.193

[12] Cui, M., Wang, H., Yao, X., Zhang, D., Xie, Y., Cui, R., & Zhang, X. (2019). Circulating microRNAs in cancer: Potential and challenge. Frontiers in Genetics, 10, 626. https://doi.org/10.3389/fgene.2019.00626

[13] Mompeon, A., Ortega-Paz, L., Vidal-Gómez, X., Costa, T. J., Pérez-Cremades, D., Garcia-Blas, S., et al. (2020). Disparate miRNA expression in serum and plasma of patients with acute myocardial infarction: A systematic and paired comparative analysis. Scientific Reports, 10(1), 5373. https://doi.org/10.1038/s41598-020-61507-z

[14] Kok, M. G. M., De Ronde, M. W. J., Moerland, P. D., Ruijter, J. M., Creemers, E. E., & Pinto-Sietsma, S. J. (2018). Small sample sizes in high-throughput miRNA screens: A common pitfall for the identification of

miRNA biomarkers. Biomolecular Detection and Quantification, 15, 1–5. https://doi.org/10.1016/j.bdq.2017.11.002

[15] Seputra, K. P., Purnomo, B. B., Susianti, H., Kalim, H., & Purnomo, A. F. (2021). miRNA-21 as reliable serum diagnostic biomarker candidate for metastatic progressive prostate cancer: Meta-analysis approach. Medical Archives, 75(5), 347–350. https://doi.org/10.5455/medarh.2021.75.347-350

[16] Fredsøe, J., Rasmussen, A. K., Mouritzen, P., Bjerre, M. T., Østergren, P., Fode, M., et al. (2020). Profiling of circulating microRNAs in prostate cancer reveals diagnostic biomarker potential. Diagnostics, 10(4), 188. https://doi.org/10.3390/diagnostics10040188

[17] Zedan, A. H., Hansen, T. F., Assenholt, J., Madsen, J. S., & Osther, P. J. (2019). Circulating miRNAs in localized/locally advanced prostate cancer patients after radical prostatectomy and radiotherapy. The Prostate, 79(4), 425–432. https://doi.org/10.1002/pros.23748

[18] He, Y., Lin, J., Kong, D., Huang, M., Xu, C., Kim, T. K., et al. (2020). Current state of circulating microRNAs as cancer biomarkers. Clinical Chemistry, 66(4), 647–661. https://doi.org/10.1093/clinchem/hvaa021

[19] Zhang, T. J., Zhou, J. D., Li, X. X., Zhang, Y. Y., & Liu, J. P. (2021). Identification of potential miRNA biomarkers for prostate cancer diagnosis using microarray data and bioinformatics analysis. Translational Andrology and Urology, 10(5), 2123–2134. https://doi.org/10.21037/tau-21-160

[20] Parol, M., Gzil, A., Bodnar, M., & Grzanka, D. (2021). Systematic review and meta-analysis of the prognostic significance of microRNAs related to metastatic and EMT process among prostate cancer patients. Journal of Translational Medicine, 19(1), 28. https://doi.org/10.1186/s12967-020-02644-x

[21] Fredsøe, J., Rasmussen, A. K., Thomsen, A. R., Mouritzen, P., Høyer, S., Borre, M., & Sørensen, K. D. (2019). Diagnostic and prognostic microRNA biomarkers for prostate cancer in cell-free urine. European Urology Focus, 4(6), 825–833. https://doi.org/10.1016/j.euf.2017.11.011

[22] Aghdam, A. M., Amiri, A., Salarinia, R., Masoudifar, A., Ghasemi, F., & Mirzaei, H. (2019). MicroRNAs as diagnostic, prognostic, and therapeutic biomarkers in prostate cancer. Critical Reviews in Eukaryotic Gene Expression, 29(2). https://doi.org/10.1615/CritRevEukaryotGeneExpr.2019025273

[23] Fabris, L., Ceder, Y., Chinnaiyan, A. M., Jenster, G. W., Sørensen, K. D., Tomlins, S. A., et al. (2016). The potential of microRNAs as prostate cancer biomarkers. European Urology, 70(2), 312–322. https://doi.org/10.1016/j.eururo.2015.12.045

[24] Armstrong, D. A., Green, B. B., Seigne, J. D., Schned, A. R., Marsit, C. J., & Christensen, B. C. (2015). MicroRNA molecular profiling from matched tumor and bio-fluids in bladder cancer. Molecular Cancer, 14, 194. https://doi.org/10.1186/s12943-015-0452-5

[25] Frydrychowicz, M., Kuszel, Ł., Dworacki, G., & Budna-Tukan, J. (2023). MicroRNA in lung cancer—A novel potential way for early diagnosis and therapy. Journal of Applied Genetics, 64(3), 459–477. https://doi.org/10.1007/s13353-023-00750-2

[26] Zhu, G., Xie, L., & Miller, D. (2017). Expression of microRNAs in thyroid carcinoma. In Bioinformatics in MicroRNA Research (pp. 261–280). Springer. https://doi.org/10.1007/978-1-4939-7046-9_19

[27] Fawzy, M. S., Ibrahiem, A. T., Bayomy, N. A., Makhdoom, A. K., Alanazi, K. S., Alanazi, A. M., et al. (2023). MicroRNA-155 and disease-related immunohistochemical parameters in cutaneous melanoma. Diagnostics, 13(6), 1205. https://doi.org/10.3390/diagnostics13061205